Article

Robust Automatic Modulation Classification Using Convolutional Deep Neural Network Based on Scalogram Information

Ahmed Mohammed Abdulkarem [1,*], Firas Abedi [2], Hayder M. A. Ghanimi [3], Sachin Kumar [4], Waleed Khalid Al-Azzawi [5], Ali Hashim Abbas [6], Ali S. Abosinnee [7], Ihab Mahdi Almaameri [8] and Ahmed Alkhayyat [9]

1 Ministry of Migration and Displaced, Baghdad 10011, Iraq
2 Department of Mathematics, College of Education, Al-Zahraa University for Women, Karbala 56001, Iraq
3 Biomedical Engineering Department, College of Engineering, University of Warith Al-Anbiyaa, Karbala 56001, Iraq
4 Big Data and Machine Learning Lab, South Ural State University, 454080 Chelyabinsk, Russia
5 Department of Medical Instruments Engineering Techniques, Al-Farahidi University, Baghdad 10011, Iraq
6 College of Information Technology, Imam Ja'afar Al-Sadiq University, Al-Muthanna 66002, Iraq
7 Altoosi University College, Najaf 54001, Iraq
8 Department of Automation and Applied Informatics, Budapest University of Technology and Economics, 1111 Budapest, Hungary
9 Faculty of Engineering, The Islamic University, Najaf 54001, Iraq
* Correspondence: iahmed215@gmail.com

Abstract: This study proposed a two-stage method, which combines a convolutional neural network (CNN) with the continuous wavelet transform (CWT) for multiclass modulation classification. The modulation signals' time-frequency information was first extracted using CWT as a data source. The convolutional neural network was fed input from 2D pictures. The second step included feeding the proposed algorithm the 2D time-frequency information it had obtained in order to classify the different kinds of modulations. Six different types of modulations, including amplitude-shift keying (*ASK*), phase-shift keying (*PSK*), frequency-shift keying (*FSK*), quadrature amplitude-shift keying (QASK), quadrature phase-shift keying (QPSK), and quadrature frequency-shift keying (QFSK), are automatically recognized using a new digital modulation classification model between 0 and 25 dB SNRs. Modulation types are used in satellite communication, underwater communication, and military communication. In comparison with earlier research, the recommended convolutional neural network learning model performs better in the presence of varying noise levels.

Keywords: modulation; deep learning; wavelet transform; multiclass classification

1. Introduction

The varieties of modulation schemes employed in wireless communication are diversifying, resulting in a more complex communication environment. Wireless communication technology is always developing. As a consequence, it is becoming more and more important to have the ability to swiftly and automatically evaluate and identify communication signals. Automated modulation categorization (AMC) is a middle step in blind signal processing in several fields, including cognitive radios [1] and SDRs [2]. There are two kinds of AMC [3]. First, to identify the potential categories of received signals, the probability function of the received signals is calculated under various hypotheses, and the results are compared with a predetermined threshold. Bayesian LB techniques often have significant sensitivity to unknown channel conditions, require substantial prior information, or are computationally demanding [4–6]. The FB approaches, which can be applied with a lower level of computer complexity, can find suboptimal solutions. Analyzing the properties

of the received signals allows for the determination of the modulation type. Without a doubt, high-quality features may provide reliable performance at a reasonable price. Recent research [7] has previously looked at some of these properties, including WT [8], cyclostationary features [9], and higher-order cumulants [10]. Support vector machines (SVMs) [11] and D-Trees [12], as well as Random Forests (RFs) [13] and KNNs [14], were frequently used for AMC systems in earlier studies. Unfortunately, these approaches are time-consuming since the extraction of handmade features requires in-depth technical knowledge and domain experience.

Deep learning (DL) has recently received a lot of attention due to its success in a number of applications, including speech recognition [15], emotion analysis [16], and computer vision [17]. In contrast to conventional data-analysis and processing techniques, the DL's capacity to automatically represent complex, high-dimensional data without the need for manual features is of critical relevance [18]. Because of this, we have noticed it encroaching on other domains, such as communications [19]. It is significant to note that some engineers have completed AMC assignments using DL with success. So far, several methods have been presented using several different techniques based on deep learning, including LSTM networks [20–23], deep convolutional networks [21,24,25], RNN [26,27], etc. To clearly define the complicated relationships of time-correlated signals across Rayleigh fading channels, along with different additive noise circumstances, an RNN-based AMC technique is examined in [28]. A sophisticated RNN architecture, known as the long short-term memory (LSTM) network [29], has been made particularly for learning the long-term dependencies in the time domain of signals with varying-length modulation. CNNs are capable of extracting more significant discriminating features from multiscale feature representations for the multiclass classification challenge when compared to RNNs and LSTM. In the newest 24-modulation DeepSig dataset, a compact CNN combining numerous residual convolutional stacks, used to gather more relevant information from multilevel representational feature maps, greatly increases the classification rate. Without feature engineering expertise, DL outperforms ML in recognition performance [30]. For network training and classification tasks, the authors in [31] employed constellation diagrams and the AlexNet CNN model. Additionally, the Caffe framework was used throughout the whole modulation classification process. Based on ACGAN, data augmentation was used in [32]. Nevertheless, Peng et al. Images with grid-like topologies were created using two pretrained models for AMC (AlexNet and GoogLeNet) by [33]. Only the additive white Gaussian noise signal model, which includes several time-frequency modifications, is useful when using feature fusion to enhance performance [34]. Despite the fact that each of these methods modifies AMC for well-researched picture-identification problems in some way, they all require an intricate image-processing stage.

The literature demonstrates that the AMC issue is solved using a broad range of feature extraction and selection techniques, as well as machine learning models. Without any prior knowledge of feature engineering, DL outperforms ML in recognition performance [35,36]. However, most of the current AMC methods perform poorly when several standard convolutional layer structures are added to a heavily deep network architecture. This occurs because extracted feature maps are represented ineffectively and trainable parameters are expensive. These techniques also need a lot of training time. AMC based on scalogram images and a deep convolutional neural network is explicitly presented in this paper. The CNN architecture automatically identified the modulation types after receiving the scalogram pictures created by the CWT approach, which is used to extract 2D data from modulated signals. The described methodology effectively utilizes deep convolutional networks to address AMC difficulties (ConvNet). For robust modulation classification against channel impairments, a well-performing and cost-efficient AMC system based on CWT transform is presented.

As an innovation in this work, the combination of feature visualization with the help of CWT transformation with deep convolutional neural networks has been used. This approach was chosen because, by visualizing the features with the help of scalogram

transformation and sending these features to the deep convolutional network, the ability to recognize patterns related to each modulation in the convolutional network increases.

The contributions of the presented study are as follows:

- 2D-scalogram images are used in order to automatically detect modulation type.
- CWT-based scalogram images are used for the visualization of modulation features in order to increase the performance of the proposed method.
- The CNN architecture is proposed to automatically classify scalogram images.
- Simulation results indicate that the presented model showed better accuracy compared to other methods.

This article is divided into five parts. Section 2 addresses both the materials and the process. The model under discussion is covered in further depth in Section 3. The research results are presented in Section 4. Section 5 summarizes the results and makes recommendations for further study directions.

2. Materials and Methods

2.1. The Formulation of ASK, FSK, and PSK

A type of digital transmission in which the digital baseband signal is changed into a band-restricted high-frequency passband signal is known as a digital passband modulation. Transition bands may be modulated using *ASK, FSK*, or *PSK*.

a. Amplitude-shift keying: The identical frequency carriers in A_1 and A_2 carry bits 0 and 1 of the baseband signal.
b. Frequency-shift keying: Bits 0 and 1 of the baseband signal are modulated using the frequency-shift keying (*FSK*) technique. Two frequencies with the same amplitude are used in *FSK*.
c. Phase-shift keying: *PSK* modulation uses phase variations of the same amplitude and frequency to modify baseband signal bits 0 and 1.
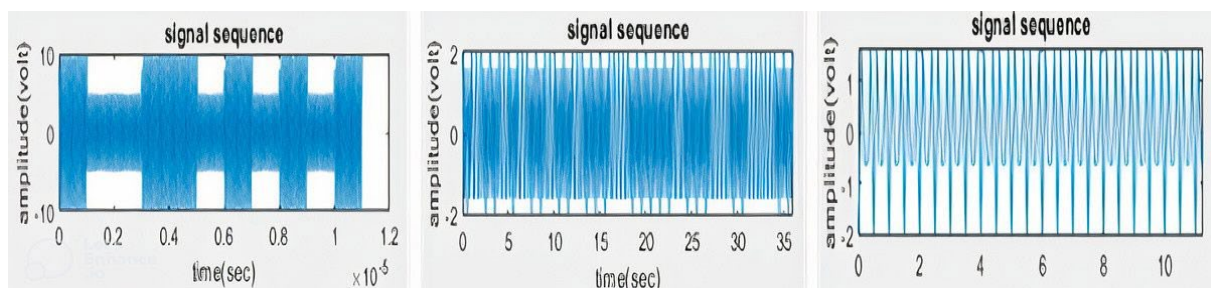
The basic modulation formulae for *ASK, FSK*, and *PSK* are listed here:

$$X_{m_{ASK}}(t) = A_m \cos \omega_c t \tag{1}$$

$$X_{m_{PSK}}(t) = A \cos(\omega_c t + \theta_m) \tag{2}$$

$$X_{m_{FSK}}(t) = A \cos(\omega_{c_m} t) \tag{3}$$

The data has been distorted in accordance with the SNR ratio for binary-10110100, which is data with a decimal value of 180, as illustrated in the diagrams for binary-10110100 digital modulation (Figure 1).

Figure 1. Examples of *ASK, FSK,* and *PSK* modulation for a string bit of 10110100.

2.2. The Formulation of QASK, QFSK, and QPSK

Multilevel transmission may be achieved by varying the amplitude, frequency, or phase of the carrier between more than two distinct values. The throughput of data transmission may be increased by having numerous carriers, as opposed to only one. Depending on the kind of modulation utilized, the carrier for the M-piece symbol may

have variable amplitude (MASK), frequency (MFSK), or phase values [37]. The binary information signal's bits are often separated into groups, each of which receives a distinct carrier. The bit group's amount of information is sent by this carrier. Multiple-level modulations often use the modulations QASK, OFSK, or OPSK. These modulations, which send out two bits at once, quadruple the transmission speed. The data transmission rate is significantly boosted with the addition of 8, 16, and 32 carriers. Moreover, as the number of carriers increases, the complexity of the demodulator circuits must also increase. Figure 2 illustrates the frequency *ASK*, *FSK*, and *PSK* modulation with AWGN in 5 dB SNR.
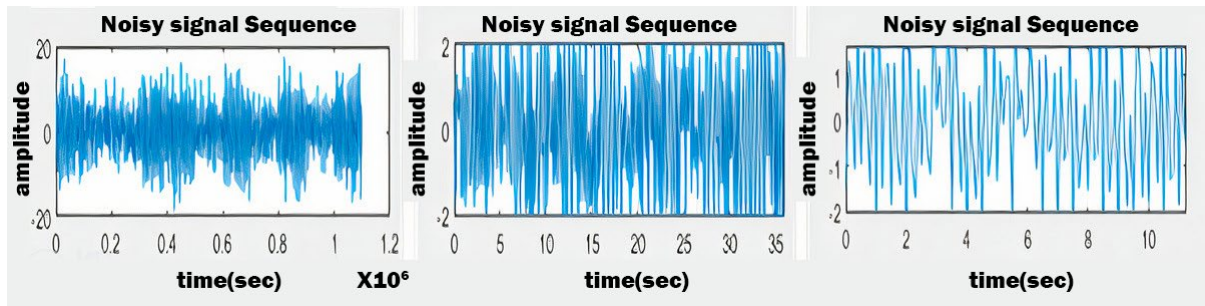

Figure 2. Examples of *ASK*, *FSK*, and *PSK* modulation with AWGN in 5 dB SNR for a string bit of 10110100.

Figure 3 illustrates binary data ranging from 0 to 255 for quadrat-type modulations, while Figure 4 illustrates corrupted signals with SNR = 5 dB noise.
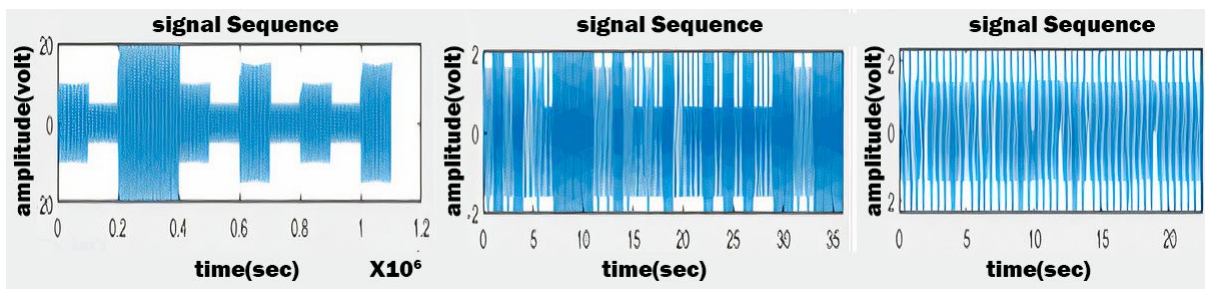

Figure 3. Examples of QASK, QFSK, and QPSK modulation for a string bit of 10110100.
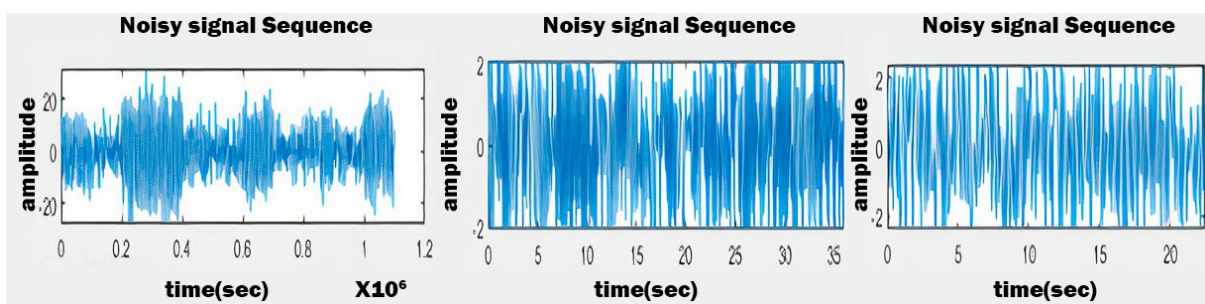
Figure 4. Examples of QASK, QFSK, and QPSK modulation with AWGN in 5 dB SNR for a string bit of 10110100.

3. The Proposed Method

This study presents a novel method for the categorization of modulation signals with noise levels ranging from 0 to 25 dB. Before the time-frequency information was extracted, these modulated signals were originally subjected to CWT. The time-frequency data that had been retrieved were first input into the CNN and fully connected layers of the deep

neural network. We will present each stage of the suggested plan in the section that follows. The flowchart for the suggested technique is shown in Figure 5.
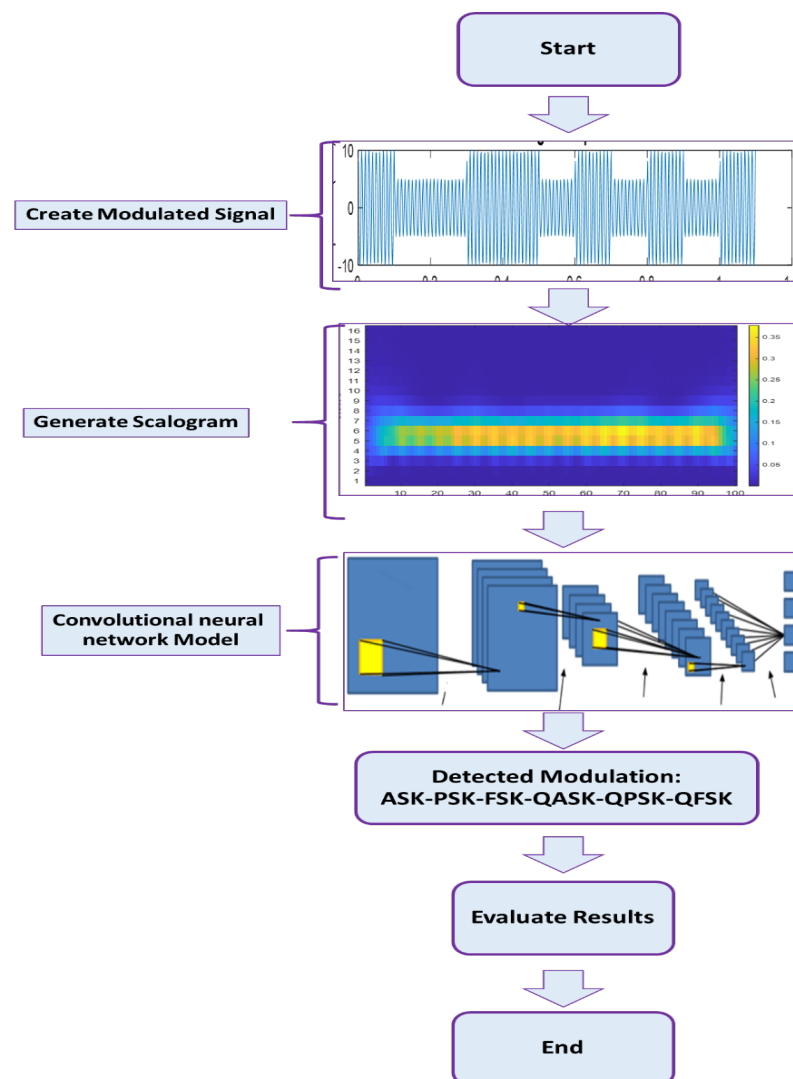
Figure 5. Diagram of the proposed method.

3.1. The Continuous Wavelet Transform (CWT)

When the continuous wavelet transform is used to analyze signals whose frequency changes over time, a time-frequency diagram is produced. The technique used to convert to the time-frequency domain is crucial in pattern-recognition techniques. For this transformation, the wavelet transform is well suited because nonstationary signals, such as EEG, ECG, and EMG, may be effectively transformed using this technique [38,39]. The signal is changed using wavelet functions, such as Daubechies, Morlet, Symlet, and Gaussian in a wavelet transform.

A signal's CWT may be expressed as:

$$Z(a.b) = \frac{1}{\sqrt{a}} \int_{-\infty}^{\infty} s(t)\psi^*\left(\frac{t-b}{a}\right) dt \qquad (4)$$

where (*t*) is a signal with finite energy, ψ^* is the mother wavelet's complex conjugate, and *a* and *b* are parameters that affect the wavelet's scaling and translation, respectively. Smaller scale values cause the wavelet to contract and disclose high frequencies in the signal, whereas larger (scale) values cause the wavelet to expand in time and show low-frequency

information in the signal [40]. By constantly changing the a and b variables along the range of scales and lengths of the signal, respectively, the continuous wavelet transform is computed.

Similar to a spectrogram made with a quick Fourier transform, a scalogram is a visual depiction of a signal's CWT (STFT). By permitting variable-size analysis windows at different frequencies, the CWT effectively outperforms the STFT in terms of temporal and frequency resolution. The frequencies that are present at various points in the signals' scalograms are evident.

3.2. Convolutional Neural Network Architecture

The second kind of neural architecture that is often used is CNN. The two main distinctions between CNN and ANN are the architecture and input data. In ANN, numerical values are employed, but in CNN, pictures are used. A collection of pixels with the dimensions w, h, and d make up an image (I). Images are sized, first by their width and height, and then by their depth. The color model used affects how deep an image seems. For example, d is equal to three in the case of the three-color RGB (Red–Green–Blue) scheme.

The architecture of the neural model consists of fully connected layers, convolution, and pooling. Convolutional filtering layers change the picture by emphasizing and extracting certain elements, which is accomplished by the convolution operation (a star operation *) between the filter k (a matrix of size $p \times p$) and the image $I_{x,y}$ (for each individual pixel in the position (x, y)):

$$k * I_{x,y} = \sum_{i=1}^{p} \sum_{j=1}^{p} k_{i,j} . I_{x+i-1,\, y+j-1} + b_1 \tag{5}$$

where b_1 is a bias. The pooling layer is used to reduce the image's file size. To analyze each pixel and its surroundings, the function $\omega(.)$ is employed (such as minimum, maximum, or average). The pixel that performs the function is added to the reduced picture $\omega(.)$. It can be expressed in the following way so as to maximize its utility:

$$\omega(I_{x,y}) = \max_{i,j \in \{-1,0,1\}} I_{x-i,y-j} \tag{6}$$

Image resizing may be calculated as $\frac{w-k}{s+1} \times \frac{h-k}{s+1}$, where s is a kernel shift (the size of neighborhood). These two layers may be used repeatedly before the FC layer, which is the last kind of layer. This neural network has a number of hidden layers and a single output layer (similar to ANN).

Our CNN model's structure is shown in Figure 6. As can be observed, this structure is made up of convolutional layers, two pooling layers, and a fully connected layer where classification is performed using the output from the second pooling layer. Six probability values are created for each of the six classes of generated modulation by our CNN after it analyses a scalogram picture.
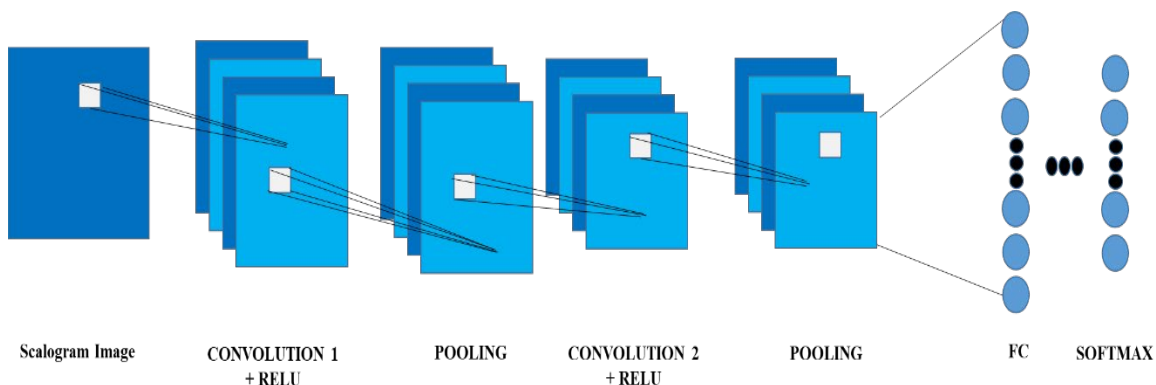

Figure 6. Structure of CNN model in this work.

4. Experimental Results

We used the CWT and deep convolutional neural network (CNN) to analyze the digital modulation categorization method. The modulation techniques used to encrypt decimal data in the range of 1 to 255 were many. MATLAB was used to create a total of six distinct SNR rates, each with a 5 dB increase, in a range from 0 dB to 25 dB.

Two different experimental conditions were created for the digital modulation categorization task. In the first experiment, a variety of SNR rates were used to evaluate the classification accuracy of the proposed model. This experiment was run five times, raising the SNR rate from 0 dB to 25 dB in 5-decibel increments, for each class of 255 samples. The information from each grade level was then compared with the others. The second experiment produced 1530 samples, with SNRs ranging from 0 to 25 dB for each class. Thus, 9180 spectrogram pictures were used to feed the suggested model. We also compared the outcomes of every experiment with one another.

Several preprocessing techniques were applied to the scalogram pictures. To eliminate any undesirable white areas, the acquired standard CWT pictures were first automatically cropped. Next, the resolutions were decreased from $657 \times 535 \times 3$ to $227 \times 227 \times 3$ pixels. This made it possible to focus on certain areas of interest in the scalogram pictures.

All training was carried out using MATLAB (2021a) and an NVIDIA graphics card (8 GB onboard RAM). We examined the model's classification ability at different SNR rates between 0 and 25 decibels (dB) in terms of our prior results. As a result, for each class, only 255 scalogram images with a single SNR rate were taken into account. To put it another way, a total of 1530 spectrogram pictures were used to feed input to the CNN model. Experiments on the modulation classification issue were carried out by randomly dividing the dataset into training (70%) and testing (30%) groups.

The suggested model contains a diagonal pattern in the confusion matrix for modulation-type recognition. It highlights the model under consideration's high level of categorization accuracy. The results of the experiment are reported in Table 1, as a function of the SNR rates. The total accuracy of all SNRs comes out to be over 99.9, indicating that the suggested approach is noise resistant.

Table 1. The proposed model's accuracy when different SNR rates are considered independently.

Class	SNR						
	0 dB	**5 dB**	**10 dB**	**15 dB**	**20 dB**	**25 dB**	**Avg. Acc**
ASK (Proposed)	99.84	99.88	99.90	99.91	99.93	99.97	99.90
FSK (Proposed)	99.58	99.60	99.70	99.91	99.94	99.94	99.77
PSK (Proposed)	99.99	99.99	99.99	100	100	100	99.99
QASK (Proposed)	99.99	99.99	99.99	100	100	100	99.99
QFSK (Proposed)	99.99	99.99	99.99	100	100	100	99.99
QPSK (Proposed)	99.99	99.99	99.99	100	100	100	99.99
Avg. ACC (Proposed)	99.90	99.91	99.92	99.97	99.978	99.98	99.938

Equations (7)–(10) are used to compute accuracy, precision, recall, and *F*1-score measurements in order to assess the model's effectiveness in the sequence of 7, 8, 9, and 10. These measurements are computed using the true positive (TP), false negative (FN), false positive (FP), and true negative (TN) indices. TP and TN reflect the number of positive and negative samples that were properly identified, while FP and FN reflect the number of positive and negative samples that were incorrectly classified.

$$Accuracy = \left(\frac{total\ number\ of\ correct\ samples}{number\ of\ total\ samples} \right)_{for\ i^{th}class} \tag{7}$$

$$Precision = \left(\frac{true\ positives}{true\ positives + false\ positives} \right)_{for\ i^{th}class} \tag{8}$$

$$Recall = \left(\frac{true\ positives}{true\ positives + false\ positives} \right)_{for\ i^{th}class} \tag{9}$$

$$F1 - score = \left(2 \times \frac{precision \times recall}{precision + recall} \right)_{for\ i^{th}class} \tag{10}$$

A total of 2000 scalograms were input into the suggested model. To ensure that the findings could be used generally, the recommended model was also trained and evaluated using the 10-fold cross-validation method. We divided the dataset into 10 groups to provide a more specific illustration. A tiny sample of the data was tested, and the remaining nine portions were utilized to train the proposed model. This process was carried out 10 times.

We utilized a confusion matrix to measure the model's performance for the digital modulation classification problem. The resultant confusion matrix is shown in Figure 7. Table 2 displays the classification results for each class of the confusion matrix. In other words, the classification performance of the suggested model was good.

Figure 7. Confusion matrix of categorization results, including all SNR rates in each class.

Table 2. The proposed model's results covered all SNR rates in each class.

Class	Accuracy	Precision	Recall	*F*-Score
ASK (Proposed)	99.90	99.80	99.90	99.93
FSK (Proposed)	99.77	99.49	99.9	99.69
PSK (Proposed)	99.99	99.99	99.99	99.99
QASK (Proposed)	99.99	99.99	99.99	99.99
QFSK (Proposed)	99.99	99.90	99.61	99.75
QPSK (Proposed)	99.99	99.99	99.80	99.88
Avg. (Proposed)	99.938	99.87	99.865	99.86

Table 2 lists the outcomes of Experiment 2. The overall accuracy, precision, recall, and *F*1-score for the proposed model are 99.938%, 99.87%, 99.865%, and 99.867%, respectively. With a classification accuracy of 99.99%, *PSK* is the most accurately identified modulation type, while *FSK* has the lowest classification accuracy at 99.77%. The experimental results show that the recommended model can successfully carry out the modulation categorization task.

As can be seen in Table 2, the accuracy of the proposed method increased with the increase of SNR. The reason for this is that, by increasing the SNR, the signal power is

increased, and as a result, the effect of the noise decreases, so it becomes easier to detect the type of modulation, and the detection accuracy increases.

We have created a novel model for classifying different forms of digital modulations based on CWT and deep convolutional neural networks (CNN). Our data source was the CWT, which creates scalograms.

We tried to use the VGG-16, VGG-19, and GoogLeNet for well over an hour. Figure 8, Table 3 compared with the different CNN architectures on the digital modulation categorization problem, presents this information, and it is clear to see that the suggested approach is, on average, quicker and more accurate than all other methods.
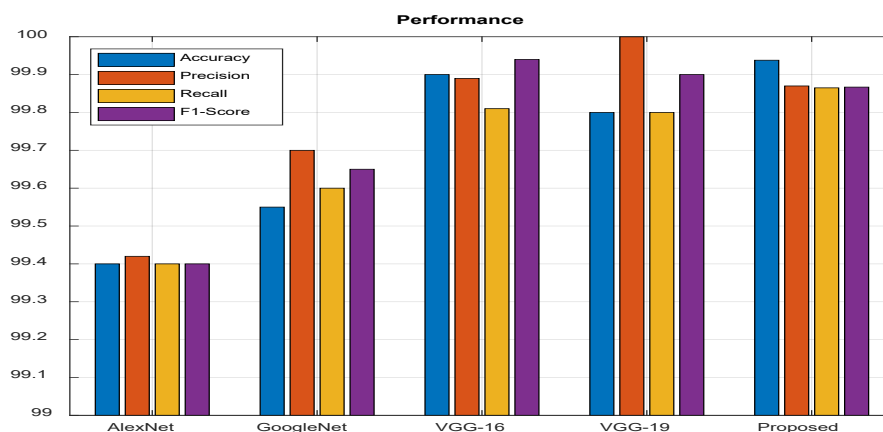
Figure 8. The performance of the pre-trained models and the proposed model.

Table 3. The proposed method is compared with the different CNN architectures on the digital modulation categorization problem.

Metrics	AlexNet	VGG-16	VGG-19	GoogLenet	Proposed
Accuracy	99.40	99.9	99.90	99.56	99.93
Precision	99.40	99.89	100	99.78	99.87
Recall	99.40	99.81	99.90	99.67	99.86
F1-Score	99.40	99.94	99.95	99.73	99.86
Time (min)	27.2	206.1	240.5	217.5	6.3

Time: The amount of time that was required during the training of the network is only equivalent to one training epoch.

We compared the proposed method against a number of previously trained CNN-based models for categorizing digital modulation. Table 4 demonstrates that the CNN models of proposed method were successful in achieving a high degree of classification accuracy (over 99% accuracy).

Table 4. Compare the proposed method against a number of previously trained CNN.

No	Title	Year	Ref	Accuracy
1	Artificial Intelligence-Driven Real-Time Automatic Modulation Classification Scheme for Next-Generation Cellular Networks.	2021	[1]	**97**
2	Machine Learning Based Automatic Modulation Recognition for Wireless Communications: A Comprehensive Survey	2021	[3]	**99**
3	Faster Maximum-Likelihood Modulation Classification in Flat Fading Non-Gaussian Channels	2019	[4]	**95**
4	Deep Convolutional Neural Network with Wavelet Decomposition for Automatic Modulation Classification	2020	[9]	**96**
5	Deep Learning-Based Robust Automatic Modulation Classification for Cognitive Radio Networks	2021	[19]	**98.7**
6	An Efficient CNN Architecture for Robust Automatic Modulation Classification	2020	[32]	**93**

5. Conclusions

In this study, a deep convolutional neural network (CNN) model for classifying different forms of digital modulation is presented. In order to assess the model's durability at different SNR rates, spanning from 0 dB to 25 dB, we first used a transfer learning technique. These results allowed us to draw the conclusion that the model can categorize various modulation types appropriately. The effectiveness of the model was assessed using all six SNR rates. The experiment's findings demonstrate that the modulation types can be determined using the CNN model. The model's classifications are accurate to a level greater than 99%. On the other hand, we contrasted GoogLeNet's performance on the same task with that of other popular CNN models. The suggested strategy surpassed all others in terms of accuracy and efficiency, as well as training time, when the different CNN models were compared. Using the hybrid methodology we suggested, we have had tremendous success categorizing digital modulation signals. We may use this application in conjunction with the newly suggested communication hardware to recognize modulation signals in the future. This capacity is necessary for both the real-time demodulation and the automated detection of this kind of modulated signal. To improve the performance of the proposed method in future work, feature-selection methods, such as (multivariate ridge regression) MRR and (Neighbourhood Component Analysis) NCA, could be used to select the optimal subset of features. These methods can increase the accuracy and speed of detection by removing the redundancies between the feature vectors.

Author Contributions: Data curation, A.M.A.; Formal analysis, A.M.A., H.M.A.G. and A.A.; Funding acquisition and Visualization, F.A.; Methodology, W.K.A.-A.; Resources, A.H.A.; Supervision, S.K.; Visualization, I.M.A.; Writing—original draft, A.M.A., A.S.A. and A.A.; Writing—review & editing, S.K. All authors have read and agreed to the published version of the manuscript.

Conflicts of Interest: The authors declare no conflict of interest.

References

1.　Kaleem, Z.; Ali, M.; Ahmad, I.; Khalid, W.; Alkhayyat, A.; Jamalipour, A. Artificial Intelligence-Driven Real-Time Automatic Modulation Classification Scheme for Next-Generation Cellular Networks. *IEEE Access* **2021**, *9*, 155584–155597. [CrossRef]
2.　Marey, M.; Mostafa, H. Turbo Modulation Identification Algorithm for OFDM Software-Defined Radios. *IEEE Commun. Lett.* **2021**, *25*, 1707–1711. [CrossRef]
3.　Jdid, B.; Hassan, K.; Dayoub, I.; Lim, W.H.; Mokayef, M. Machine Learning Based Automatic Modulation Recognition for Wireless Communications: A Comprehensive Survey. *IEEE Access* **2021**, *9*, 57851–57873. [CrossRef]
4.　Chen, W.; Xie, Z.; Ma, L.; Liu, J.; Liang, X. A Faster Maximum-Likelihood Modulation Classification in Flat Fading Non-Gaussian Channels. *IEEE Commun. Lett.* **2019**, *23*, 454–457. [CrossRef]
5.　Abu-Romoh, M.; Aboutaleb, A.; Rezki, Z. Automatic Modulation Classification Using Moments and Likelihood Maximization. *IEEE Commun. Lett.* **2018**, *22*, 938–941. [CrossRef]
6.　Han, L.; Gao, F.; Li, Z.; Dobre, O.A. Low Complexity Automatic Modulation Classification Based on Order-Statistics. *IEEE Trans. Wirel. Commun.* **2016**, *16*, 400–411. [CrossRef]
7.　Peng, S.; Sun, S.; Yao, Y.-D. A survey of modulation classification using deep learning: Signal representation and data preprocessing. *IEEE Trans. Neural Netw. Learn. Syst.* **2021**. [CrossRef]
8.　Wang, H.; Ding, W.; Zhang, D.; Zhang, B. Deep Convolutional Neural Network with Wavelet Decomposition for Automatic Modulation Classification. In Proceedings of the 2020 15th IEEE Conference on Industrial Electronics and Applications (ICIEA), Kristiansand, Norway, 9–13 November 2020.
9.　Ma, J.; Qiu, T. Automatic Modulation Classification Using Cyclic Correntropy Spectrum in Impulsive Noise. *IEEE Wirel. Commun. Lett.* **2018**, *8*, 440–443. [CrossRef]
10.　Lee, S.H.; Kim, K.-Y.; Shin, Y. Effective Feature Selection Method for Deep Learning-Based Automatic Modulation Classification Scheme Using Higher-Order Statistics. *Appl. Sci.* **2020**, *10*, 588. [CrossRef]
11.　Lv, J.; Zhang, L.; Teng, X. A modulation classification based on SVM. In Proceedings of the 2016 15th International Conference on Optical Communications and Networks (ICOCN), Hangzhou, China, 24–27 September 2016.
12.　Subbarao, M.V.; Punniakodi, S. Automatic modulation recognition in cognitive radio receivers using multi-order cumulants and decision trees. *Int. J. Rec. Technol. Eng* **2018**, *7*, 61–69.
13.　Zhao, Y.; Shi, C.; Wang, D.; Chen, X.; Wang, L.; Yang, T.; Du, J. Low-Complexity and Nonlinearity-Tolerant Modulation Format Identification Using Random Forest. *IEEE Photon. Technol. Lett.* **2019**, *31*, 853–856. [CrossRef]

14. Ghauri, S.A.; Khan, S. Knn based classification of digital modulated signals. *IIUM Eng. J.* **2016**, *17*, 71–82. [CrossRef]
15. Lee, W.; Seong, J.; Ozlu, B.; Shim, B.; Marakhimov, A.; Lee, S. Biosignal Sensors and Deep Learning-Based Speech Recognition: A Review. *Sensors* **2021**, *21*, 1399. [CrossRef]
16. Kottursamy, K. A Review on Finding Efficient Approach to Detect Customer Emotion Analysis using Deep Learning Analysis. *J. Trends Comput. Sci. Smart Technol.* **2021**, *3*, 95–113. [CrossRef]
17. Zhou, R.; Liu, F.; Gravelle, C.W. Deep Learning for Modulation Recognition: A Survey with a Demonstration. *IEEE Access* **2020**, *8*, 67366–67376. [CrossRef]
18. Kim, S.-H.; Kim, J.-W.; Nwadiugwu, W.-P.; Kim, D.-S. Deep Learning-Based Robust Automatic Modulation Classification for Cognitive Radio Networks. *IEEE Access* **2021**, *9*, 92386–92393. [CrossRef]
19. Bu, K.; He, Y.; Jing, X.; Han, J. Adversarial Transfer Learning for Deep Learning Based Automatic Modulation Classification. *IEEE Signal Process. Lett.* **2020**, *27*, 880–884. [CrossRef]
20. Chen, Y.; Shao, W.; Liu, J.; Yu, L.; Qian, Z. Automatic modulation classification scheme based on LSTM with random erasing and attention mechanism. *IEEE Access* **2020**, *8*, 154290–154300. [CrossRef]
21. Zhang, Z.; Luo, H.; Wang, C.; Gan, C.; Xiang, Y. Automatic Modulation Classification Using CNN-LSTM Based Dual-Stream Structure. *IEEE Trans. Veh. Technol.* **2020**, *69*, 13521–13531. [CrossRef]
22. Xu, Q.; Yao, Z.; Tu, Y.; Chen, Y. Attention-Based Multi-component LSTM for Internet Traffic Prediction. In Proceedings of the International Conference on Neural Information Processing, Bangkok, Thailand, 18–22 November 2020.
23. Yang, Z.; Chen, L.; Zhang, H.; Yao, Z. Residual Connection based TPA-LSTM Networks for Cluster Node CPU Load Prediction. In Proceedings of the 2021 IEEE International Conference on Big Data (Big Data), Orlando, FL, USA, 15–18 December 2021.
24. Amorim, A.; Morehouse, T.; Kasilingam, D.; Zhou, R.; Magotra, N. CNN-based AMC for Internet of Underwater Things. In Proceedings of the 2021 IEEE International Midwest Symposium on Circuits and Systems (MWSCAS), Lansing, MI, USA, 8–11 August 2021.
25. Kojima, S.; Maruta, K.; Ahn, C.J. High-precision SNR estimation by CNN using PSD image for adaptive modulation and coding. In Proceedings of the 2020 IEEE 91st Vehicular Technology Conference (VTC2020-Spring), Antwerp, Belgium, 25–28 May 2020.
26. Ghasemzadeh, P.; Hempel, M.; Sharif, H. GS-QRNN: A High-Efficiency Automatic Modulation Classifier for Cognitive Radio IoT. *IEEE Internet Things J.* **2022**, *9*, 9467–9477. [CrossRef]
27. Moore, M.O.; Buehrer, R.M.; Headley, W.C. Decoupling RNN Training and Testing Observation Intervals for Spectrum Sensing Applications. *Sensors* **2022**, *22*, 4706. [CrossRef] [PubMed]
28. Rajendran, S.; Meert, W.; Giustiniano, D.; Lenders, V.; Pollin, S. Deep Learning Models for Wireless Signal Classification with Distributed Low-Cost Spectrum Sensors. *IEEE Trans. Cogn. Commun. Netw.* **2018**, *4*, 433–445. [CrossRef]
29. Hu, S.; Pei, Y.; Liang, P.P.; Liang, Y.C. Robust modulation classification under uncertain noise condition using recurrent neural network. In Proceedings of the 2018 IEEE Global Communications Conference (GLOBECOM), Abu Dhabi, United Arab Emirates, 9–13 December 2018.
30. Huynh-The, T.; Hua, C.-H.; Pham, Q.-V.; Kim, D.-S. MCNet: An Efficient CNN Architecture for Robust Automatic Modulation Classification. *IEEE Commun. Lett.* **2020**, *24*, 811–815. [CrossRef]
31. Zhang, Z.; Wang, C.; Gan, C.; Sun, S.; Wang, M. Automatic Modulation Classification Using Convolutional Neural Network with Features Fusion of SPWVD and BJD. *IEEE Trans. Signal Inf. Process. Netw.* **2019**, *5*, 469–478. [CrossRef]
32. Tang, B.; Tu, Y.; Zhang, Z.; Lin, Y. Digital signal modulation classification with data augmentation using generative adversarial nets in cognitive radio networks. *IEEE Access* **2018**, *6*, 15713–15722. [CrossRef]
33. Kumar, Y.; Sheoran, M.; Jajoo, G.; Yadav, S.K. Automatic Modulation Classification Based on Constellation Density Using Deep Learning. *IEEE Commun. Lett.* **2020**, *24*, 1275–1278. [CrossRef]
34. Han, H.; Ren, Z.; Li, L.; Zhu, Z. Automatic Modulation Classification Based on Deep Feature Fusion for High Noise Level and Large Dynamic Input. *Sensors* **2021**, *21*, 2117. [CrossRef]
35. Wang, Y.; Yang, J.; Liu, M.; Gui, G. LightAMC: Lightweight Automatic Modulation Classification via Deep Learning and Compressive Sensing. *IEEE Trans. Veh. Technol.* **2020**, *69*, 3491–3495. [CrossRef]
36. Lin, Y.; Tu, Y.; Dou, Z. An Improved Neural Network Pruning Technology for Automatic Modulation Classification in Edge Devices. *IEEE Trans. Veh. Technol.* **2020**, *69*, 5703–5706. [CrossRef]
37. Grewal, D.; Herhausen, D.; Ludwig, S.; Ordenes, F.V. The Future of Digital Communication Research: Considering Dynamics and Multimodality. *J. Retail.* **2021**, *98*, 224–240. [CrossRef]
38. Narin, A. Detection of Focal and Non-focal Epileptic Seizure Using Continuous Wavelet Transform-Based Scalogram Images and Pre-trained Deep Neural Networks. *IRBM* **2020**, *43*, 22–31. [CrossRef]
39. Wang, T.; Lu, C.; Sun, Y.; Yang, M.; Liu, C.; Ou, C. Automatic ECG Classification Using Continuous Wavelet Transform and Convolutional Neural Network. *Entropy* **2021**, *23*, 119. [CrossRef]
40. Meintjes, A.; Lowe, A.; Legget, M. Fundamental heart sound classification using the continuous wavelet transform and convolutional neural networks. In Proceedings of the 2018 40th Annual International Conference of the IEEE Engineering in Medicine and Biology Society (EMBC), Honolulu, HI, USA, 18–21 July 2018.